

# Systematic Workflow for Efficient Identification of Local Representative Elementary Volumes Demonstrated with Lithium-Ion Battery Cathode Microstructures

## Supporting Information

Benjamin Kellers\*, Martin P. Lautenschlaeger, Nireas Rigos,  
Julius Weinmiller, Timo Danner\*, and Arnulf Latz

The following document includes six pieces of supporting information. Table S1 summarizes the parameters used for the electrochemical simulations in the study. Figure S1 illustrates the two-point correlations for different types of material. Figures S2 to S4 show the heatmaps for the other three cut size classes. And, finally, Figure S5 contains the full curves of the charging simulations.

## Parameters of Electrochemical Simulations

Table S1: Summary of the electrochemical simulation parameters.

Parameter	Description	NMC622	Electrolyte	Separator	CBD Phase
$c^0 / \text{mol m}^{-3}$	Concentration init.	32,940	1000		
$c^{\max} / \text{mol m}^{-3}$	Concentration max.	33,000			
$D / \text{m}^2 \text{s}^{-1}$	Diffusivity	$1 \times 10^{-14}$	functional <sup>[1]</sup>		
$\kappa, \sigma / \text{S m}^{-1}$	Conductivity	$1 \times 10^{-4}$	functional <sup>[1]</sup>		0.1
$t_+ / -$	Transference number		functional <sup>[1]</sup>		
$f / -$	Activity coef.		functional <sup>[1]</sup>		
$U_0 / \text{V}$	Open-Circuit Voltage	functional			
$\varepsilon_{\text{el}} / -$	Vol. Fraction El/yte			0.87	0.5
$\tau_{\text{so}} / -$	Tortuosity Solid				1.0
$\tau_{\text{el}} / -$	Tortuosity El/yte			1.07	2.0
$i_{00} / \text{Am}^{2.5} \text{mol}^{-1.5}$	Exchange Current prefactor	$0.5 \times 10^{-5}$			

\*Correspondence: Benjamin.Kellers@dlr.de, Timo.Danner@dlr.de

## Comparison of Different Types of Microstructures

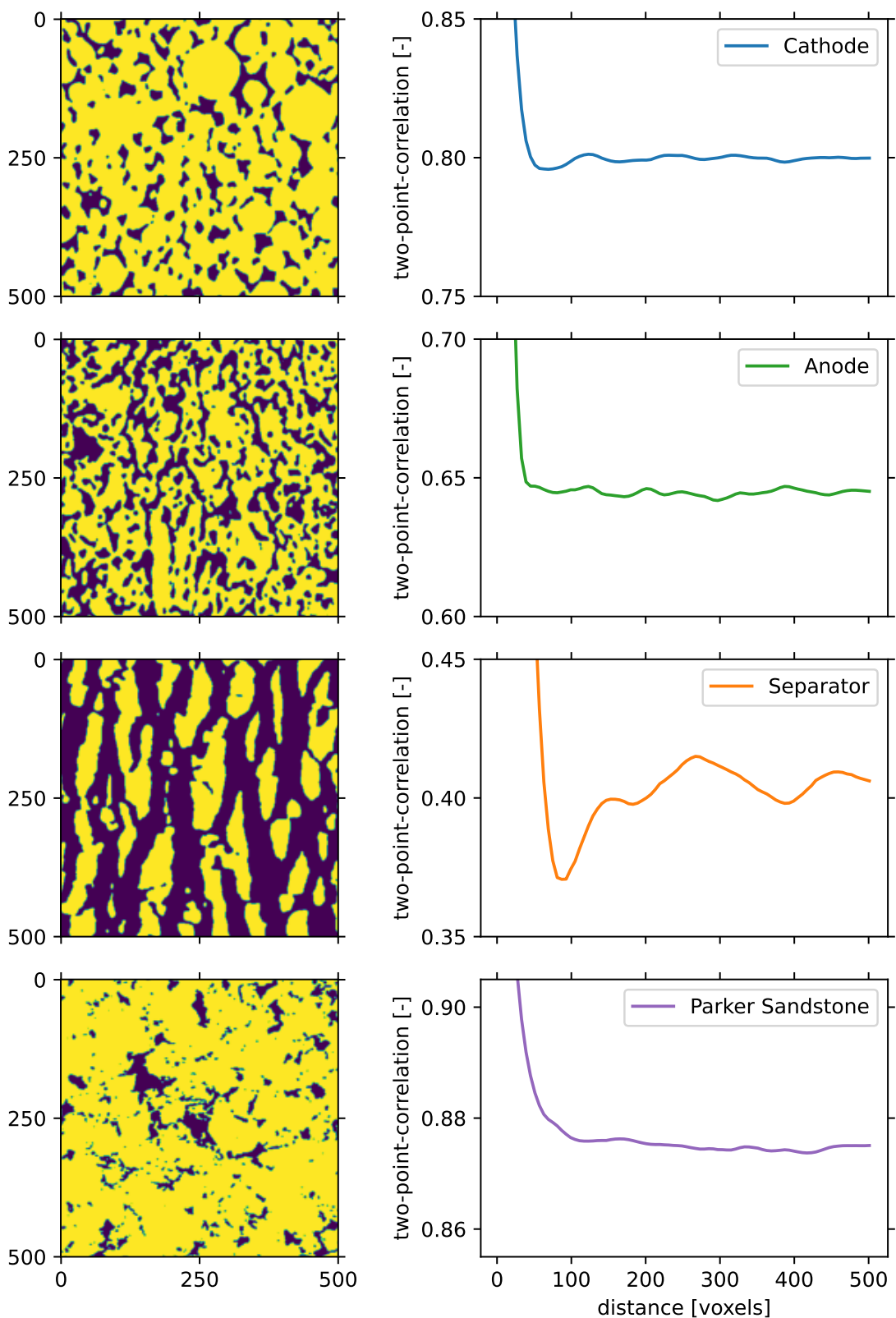


Figure S1: Two-point correlations of different materials. From top to bottom: Cathode material, anode material, battery separator, and Parker sandstone.

## Heatmaps for Cut Size Class 75

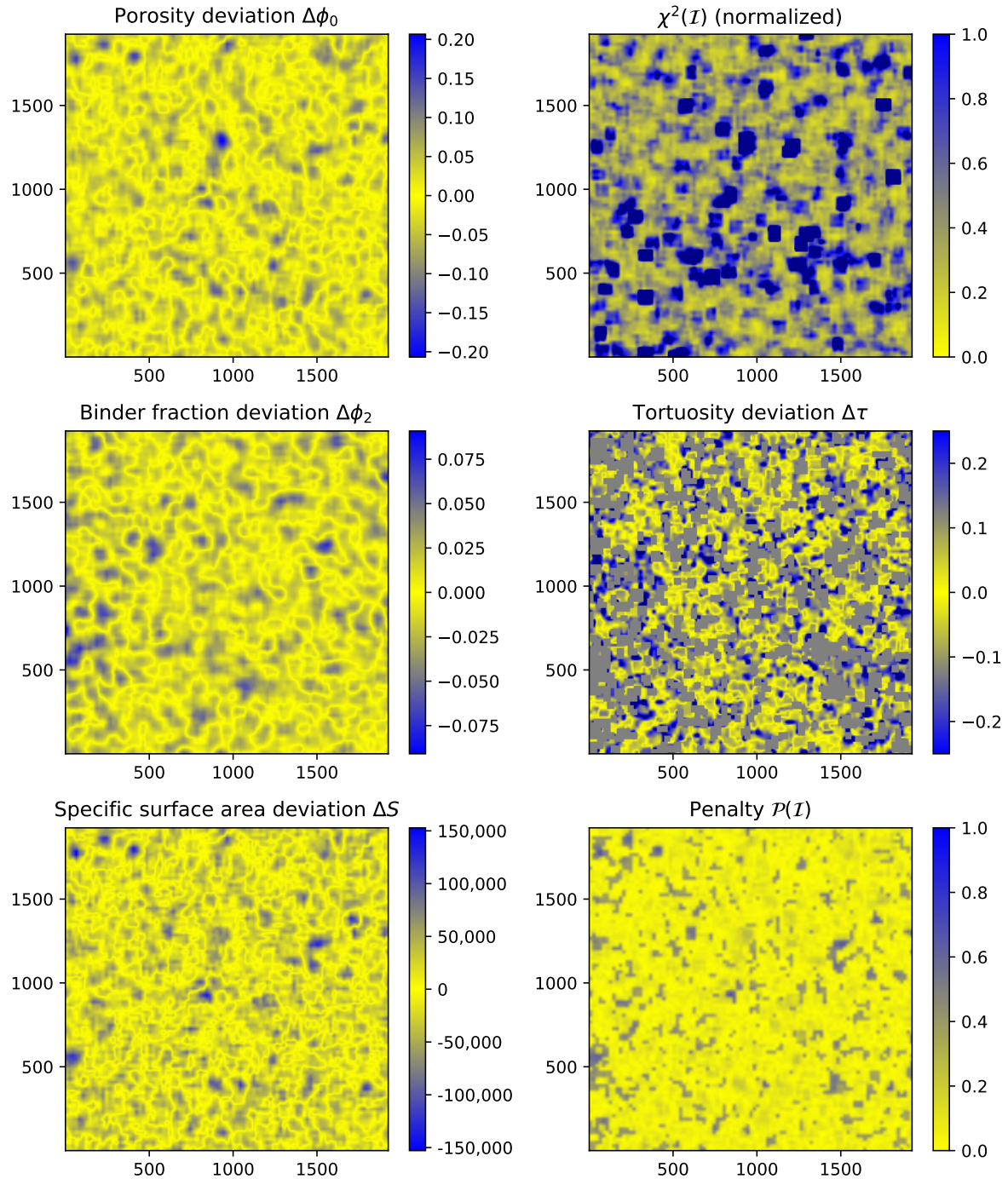


Figure S2: Deviation of local and global results of the structural influencing factors for a cut size of 75 voxels. In addition, results of the penalty function are given. Values are shown as heatmaps in the range indicated by the legend and color map. Each pixel corresponds to one window.

## Heatmaps for Cut Size Class 150

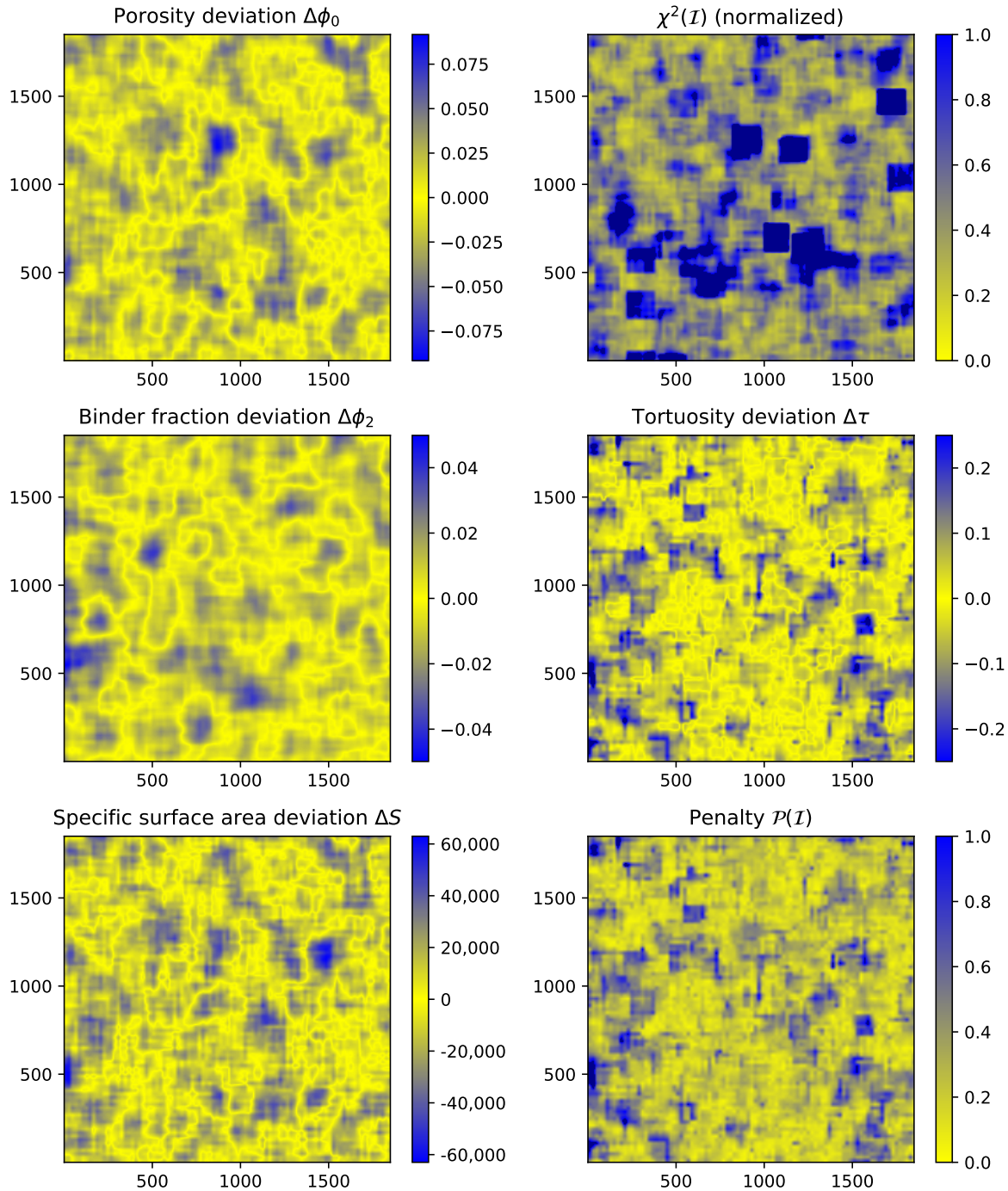


Figure S3: Deviation of local and global results of the structural influencing factors for a cut size of 150 voxels. In addition, results of the penalty function are given. Values are shown as heatmaps in the range indicated by the legend and color map. Each pixel corresponds to one window.

## Heatmaps for Cut Size Class 600

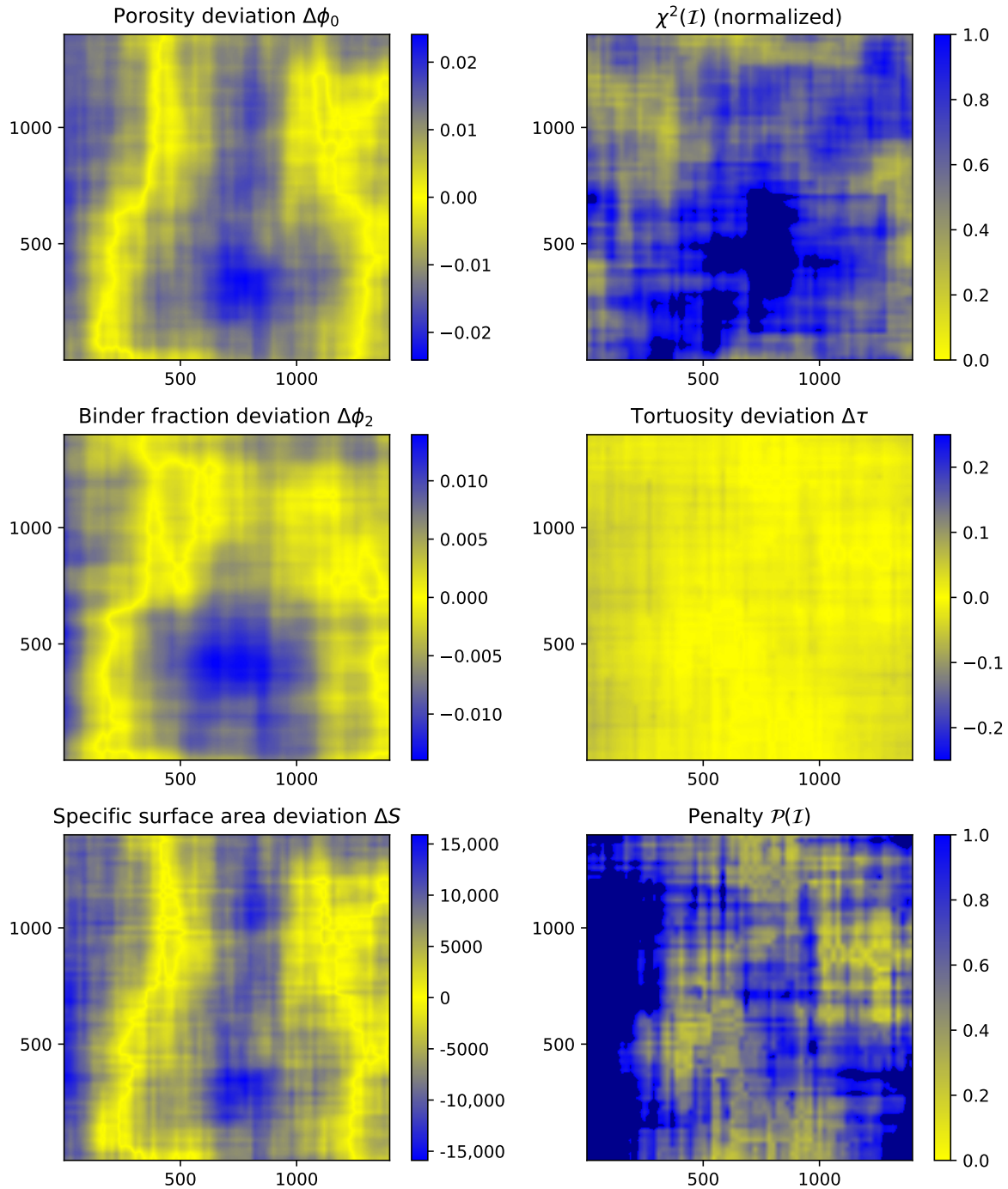


Figure S4: Deviation of local and global results of the structural influencing factors for a cut size of 600 voxels. In addition, results of the penalty function are given. Values are shown as heatmaps in the range indicated by the legend and color map. Each pixel corresponds to one window.

## Results of Charging Simulations

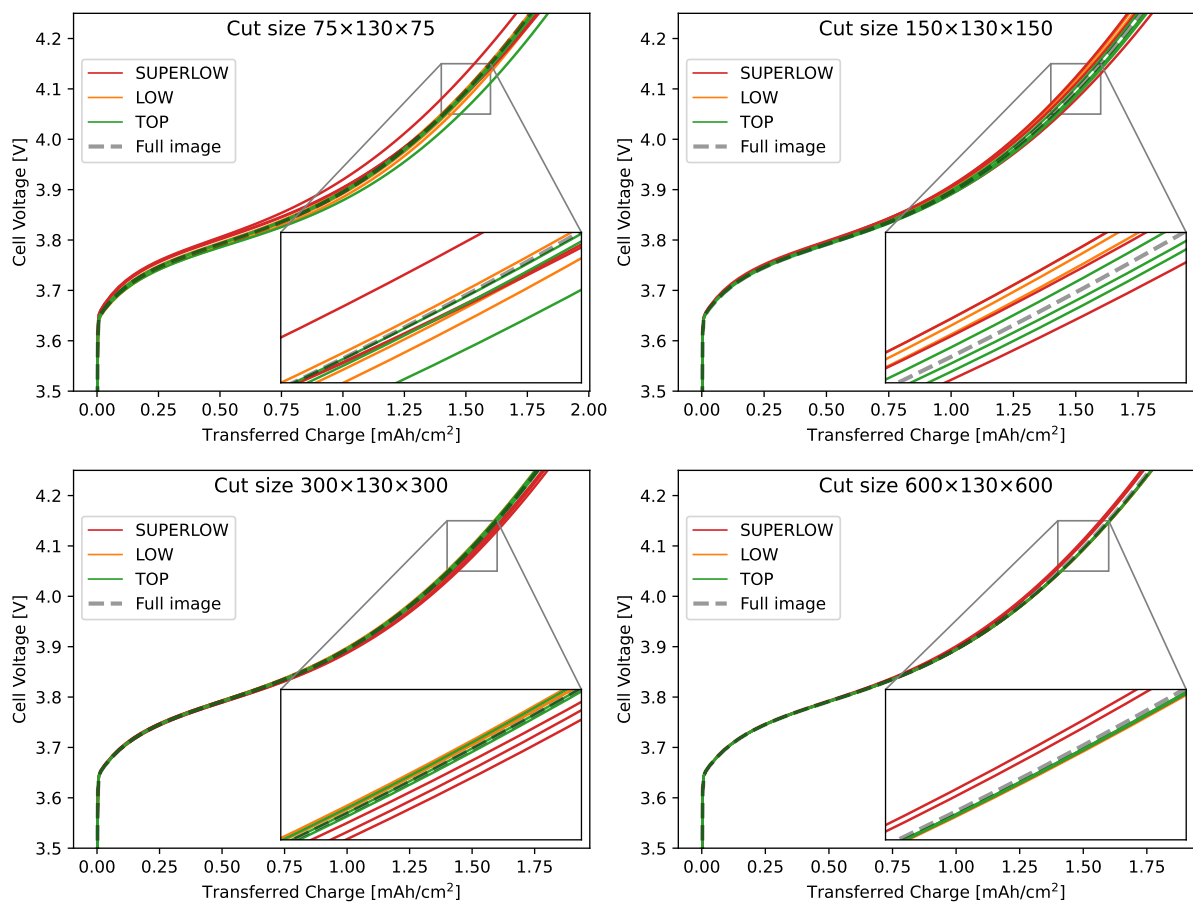


Figure S5: Full data sets of the charging simulations. The cell voltage is shown as a function of transferred charge normalized to the surface area.

## References

- [1] Vittorio De Lauri et al. "Beneficial Effects of Three-Dimensional Structured Electrodes for the Fast Charging of Lithium-Ion Batteries". In: *ACS Applied Energy Materials* 4 (12 2021), pp. 13847–13859. ISSN: 25740962. DOI: 10.1021/acsaem.1c02621.